metabolites

MDPI

Article

Toxicometabolomics Characterization of Two N1-Sulfonated Dimethyltryptamine Derivatives in Zebrafish Larvae and Human Liver S9 Fractions Using Liquid Chromatography–High-Resolution Mass Spectrometry

Prajwal Punnamraju [1,2], Sascha K. Manier [1], Selina Hemmer [1], Matthias Grill [3], Philip Schippers [1,2], Jennifer Herrmann [2] and Markus R. Meyer [1,*]

[1] Experimental and Clinical Toxicology and Pharmacology, Center for Molecular Signaling (PZMS), PharmaScienceHub (PSH), Saarland University, 66424 Homburg, Germany
[2] Helmholtz Institute for Pharmaceutical Research Saarland (HIPS), Helmholtz Centre for Infection Research (HZI), PharmaScienceHub (PSH), Saarland University, Campus E 8.1, 66123 Saarbrücken, Germany
[3] MiHKAL GmbH, Allschwil, CH-4123 Basel, Switzerland
* Correspondence: markus.meyer@uni-saarland.de

Abstract

Introduction: The availability of toxicokinetic data is critical for detecting and monitoring the intake of psychoactive substances. Timely characterization of novel psychoactive substances (NPS) is particularly important to assess their abuse potential and inform public health responses. **Methods**: Toxicometabolomics offers a powerful approach to characterize xenobiotic metabolism through high-resolution profiling of biochemical transformations. It thus allows the finding of exogenous biomarkers, such as new drug metabolites, and endogenous biomarkers, which could be indications of acute drug ingestions or sample manipulation, as well as offering information on the mode of action of drugs. In this study, we applied a liquid chromatography–high-resolution mass spectrometry workflow to investigate the toxicometabolomics of two N1-sulfonated *N*,*N*-dimethyltryptamine derivatives with potential for both therapeutic use and recreational abuse. **Results**: Zebrafish (*Danio rerio*), an increasingly valuable model for preclinical pharmacology and toxicology studies, along with pooled human liver S9 fractions were used to elucidate metabolic pathways and identify key phase I and phase II biotransformations. Furthermore, untargeted metabolomics revealed significant downregulation of L-threonine associated with compound exposure. **Conclusions**: These findings advance the current understanding of tryptamine metabolism and underscore the utility of toxicometabolomics in the analytical evaluation of NPS.

Keywords: toxicometabolomics; novel psychoactive substances; zebrafish larvae; human liver S9 fractions; liquid chromatography–high-resolution mass spectrometry

Academic Editors: Pengcheng Wang and Rheem A. Totah

Received: 14 January 2026
Revised: 9 February 2026
Accepted: 11 February 2026
Published: 14 February 2026

1. Introduction

Between 2005 and 2024, the European Monitoring Centre for Drugs and Drug Addiction (EMCDDA) reported approximately 950 new psychoactive substances (NPS), including over 50 synthetic tryptamines [1]. Due to the structural diversity of NPS and the lack of toxicokinetic information including metabolic fate, the detection of an intake is an analytical challenge. Furthermore, knowledge about the detailed mode of action and possible off target effects of drugs (of abuse) and NPS is often missing. In clinical and forensic

toxicology as well as doping control, knowledge about the toxicometabolomics of new drugs (of abuse) is important for their risk assessment in general and for monitoring their ingestion [2]. Toxicometabolomics, as a subdiscipline of metabolomics, has increasingly gained interest in toxicological studies of drugs/drugs of abuse [3–10]. The application of untargeted toxicometabolomics allows the identification of exogenous biomarkers, such as new drug metabolites, and endogenous biomarkers, which could be indications of acute drug ingestions or sample manipulation, as well as offer information on the mode of action of drugs [11–13]. Studying the metabolism allows the evaluation of the chemical modifications in their ability to enable prodrug functionality and toxicokinetic studies [14].

Danio rerio is a model organism well suited for such preclinical studies. It offers the unique advantage of being an in vivo model for which regulations on animal experimentation do not apply (under European Union Directive 2010/63/EU) up to five days post fertilization (dpf). Compared to rodent or mouse models, the ease of handling, low maintenance costs, and compliance with the 3Rs principle make it an appealing model. At three dpf, the zebrafish larvae (ZFL) develop a functional liver capable of performing phase I and phase II biotransformation, which makes it a suitable model especially for metabolism studies [15]. Moreover, it has been successfully used as a model to investigate metabolism in various studies with small molecules in the preclinical stages [16–20]. In addition to its metabolic system, its physiological and genetic similarity to humans makes it highly suitable for toxicometabolomics studies, especially when combined with comprehensive analyses using human liver S9 fractions [14].

N,*N*-dimethyltryptamine (DMT), a substituted tryptamine, is a hallucinogenic substance which has been in consumption for thousands of years, produced mainly through botanical preparations for traditional medicine or spiritual practices [21]. It is also considered to be a psychoactive compound for the treatment of various conditions in the anxiety spectrum [22]. Its simple molecular structure, low molecular weight, and hydrophobic nature allow DMT to cross the blood–brain barrier (BBB) [23]. However, DMT is not orally bioavailable due to rapid deamination by intestinal and hepatic monoamine oxidase-A (MAO-A) [24,25]. Administration in conjunction with MAO-A inhibitors is associated with negative side effects such as high blood pressure, nausea, and hyperthermia [22,26]. Therefore, structural modifications to DMT were proposed to improve the therapeutic properties. Furthermore, DMT is classified as a scheduled drug in most countries due to its adverse psychedelic effects, meaning that the possession, sale, transport, and cultivation of DMT is illegal. However, prodrugs of the molecule are typically not regulated. Therefore, these molecules have the potential to be abused for recreational use, and studying the metabolism of these molecules should allow to identify the ingestion of these compounds in clinical and forensic toxicology as well as doping control [1].

The current study should give insights into the in vivo toxicometabolomics and in vitro metabolism of two DMT derivatives—DMT esylate and DMT mesylate (Figure 1), hereafter referred to as DMT-E and DMT-M respectively, which were designed for their improved pharmacokinetic properties compared to DMT, and to potentially act as DMT prodrugs. The compounds are N_1-sulfonyltryptamine derivatives, which are known to be antagonists of the human 5-HT_6 receptor, which has been linked to various neuropsychiatric disorders [27]. It is a well-known strategy to utilize the sulfonamide moiety to impart metabolic stability to drug candidates, since sulfonamides are generally not hydrolyzed by common mammalian metabolic enzymes such as esterases or amidases, and their chemistry makes them inherently stable [28]. Therefore, it is envisioned that they are not subject to the kind of first pass metabolism observed for DMT. Cleavage of the sulfonamide group is rare, but nevertheless still enzymatically possible via a Glutathione-S-transferase mediated pathway [29], which may potentially impart prodrug character to the compounds.

Although N_1-sulfonated DMTs are not expected to function as psychedelic substances due to the blocking of the N_1 amine group key to inducing a psychedelic response [30,31], they are known to have promising therapeutic effects in cognition enhancement and memory modulation as a result of 5-HT_6 binding [32,33], which leads to their potential as substances of abuse.

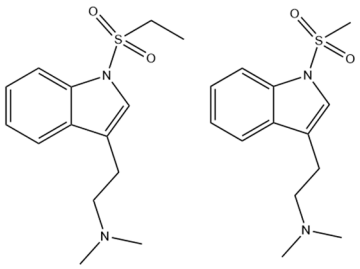

(**a**) (**b**)

Figure 1. Chemical structures of the N1-sulfonyl tryptamine derivatives analyzed in the study. (**a**) *N*,*N*-dimethyltryptamine esylate; (**b**) *N*,*N*-dimethyltryptamine mesylate.

2. Materials and Methods

2.1. Chemicals and Reagents

DMT-E and DMT-M were provided by MiHKAL GmbH (Basel, Switzerland). Dimethyl sulfoxide (DMSO) and tricaine (3-amino-benzoic acid ethyl ester) were obtained from Sigma-Aldrich (Taufkirchen, Germany). Methanol (LC-MS grade), acetonitrile (LC-MS grade), and formic acid (LC-MS grade) were from VWR (Darmstadt, Germany). NaCl, KCl, $MgSO_4$, $Ca(NO_3)_2$, and HEPES were obtained from Carl Roth (Karlsruhe, Germany). The working solutions of the compounds were freshly prepared prior to each experiment. The 24-well plates and 6-well plates were purchased from Sarstedt (Nümbrecht, Germany). ZFL of the AB wild-type line were initially obtained from the Luxembourg Center for Systems Biomedicine (Belvaux, Luxembourg). Dry small granulate food was purchased from SDS Deutschland (Limburgerhof, Germany), and Artemia cysts (>230,000 nauplii per gram) were obtained from Coralsands (Wiesbaden, Germany). NADP-Na_2, acetonitrile (LC-MS grade), and methanol (LC-MS grade) were obtained from VWR (Darmstadt, Germany), 3′-phosphoadenosine-5′-phosphosulfate (PAPS), S-(5′-adenosyl)-l-methionine (SAM), dithiothreitol (DTT), reduced glutathione (GSH), acetylcarnitine transferase (AcT), acetylcarnitine, acetyl coenzyme A (AcCoA), $MgCl_2$, K_2HPO_4, KH_2PO_4, superoxide dismutase, isocitrate dehydrogenase, isocitrate, ammonium formate, and formic acid from Sigma (Taufkirchen, Germany). Water was purified using a Millipore filtration unit (18.2 Ω × cm water resistance) from Sigma (Taufkirchen, Germany) Pooled human liver S9 fraction (pHLS9, 20 mg protein/mL, from 30 individual donors), UGT reaction mix solution A (25 mM UDP-glucuronic acid), and UGT reaction mix solution B (250 mM Tris-HCl, 40 mM $MgCl_2$, and 0.125 mg/mL alamethicin) were obtained from Corning (Amsterdam, The Netherlands). After delivery, the pHLS9 were thawed at 37 °C, aliquoted, snap-frozen in liquid nitrogen, and stored at −80 °C until use.

2.2. In Vitro Metabolism Using Pooled Liver S9 (pHLS9) Fraction

2.2.1. Sample Preparation

Investigation of the in vitro metabolism using pHLS9 was based on previous publications [34–36]. Briefly, pHLS9 was used at a final protein concentration of 2 mg/mL. The incubation was performed after a 10 min preincubation at 37 °C with 25 µg/mL alamethicin (UGT reaction mix solution B), 90 mM phosphate buffer (pH 7.4), 2.5 mM Mg^{2+}, 2.5 mM isocitrate, 0.6 mM NADP+, 0.8 U/mL isocitrate dehydrogenase, 100 U/mL superoxide

dismutase, 0.1 mM AcCoA, 2.3 mM acetyl carnitine, and 8 U/mL carnitine acetyltransferase. Subsequently, 2.5 mM UDP-glucuronic acid (UGT reaction mix solution A), 40 µM aqueous PAPS, 1.2 mM SAM, 1 mM DTT, 10 mM GSH, and 25 µM substrate in distilled water were added. The final volume of the incubation mixture was 150 µL. All given concentrations are final concentrations. Reactions were started by the addition of substrate and incubated for a maximum of 480 min. After 60 min, 60 µL of the mixture was transferred into a reaction tube and reactions were terminated by addition of 20 µL ice-cold acetonitrile containing 5 µM alpha-PVP as an internal standard. The remaining mixture was incubated for additional 7 h and then stopped by the addition of 30 µL ice-cold acetonitrile containing 5 µM alpha-PVP. Additionally, blank samples not containing pHLS9, but the according amount of phosphate buffer were incubated to identify compounds of non-metabolic origin. Blank samples not containing substrate were incubated as well. The solutions were cooled for 30 min at −18 °C, centrifuged for 2 min at 14,000× *g*, and finally 60 µL of the supernatants were transferred into an autosampler vial. One µL supernatant was injected onto the LC-HR-MS/MS system as described below. All incubations were done in duplicates.

2.2.2. Data Acquisition (LC-HRMS/MS Conditions) and Evaluation for Identification of Metabolites

The analysis was performed using a Thermo Fisher Scientific (TF, Dreieich, Germany) Dionex UltiMate 3000 RS pump consisting of a degasser, a quaternary pump, and an UltiMate Autosampler, coupled to a TF Q Exactive Plus system equipped with a heated electrospray ionization HESI-II source. Mass calibration was done prior to analysis according to the manufacturer's recommendations using external mass calibration. The conditions were set according to published procedures [34,37,38]. Gradient elution was performed on a TF Accucore Phenyl-Hexyl column (100 mm × 2.1 mm, 2.6 µm). The polar mobile phase (eluent A) consisted of 2 mM aqueous ammonium formate, containing acetonitrile (1%, *v*/*v*) and formic acid (0.1%, *v*/*v*, pH 3). Eluent B consisted of 2 mM ammonium formate dissolved in acetonitrile: methanol (1:1, *v*/*v*) containing water (1%, *v*/*v*) and formic acid (0.1%, *v*/*v*). The flow rate was set from 1 to 10 min to 500 µL/min and from 10 to 13.5 min to 800 µL/min using the following gradient: 0–1.0 min 99% A, 1–10 min to 1% A, 10–11.5 min hold 1% A, and 11.5–13.5 min hold 99% A. Samples were also analyzed using hydrophilic interaction chromatography (HILIC) as described under 2.3.4. The HESI-II source conditions were as follows: ionization mode, positive; sheath gas, 53 AU; auxiliary gas, 14 AU; sweep gas, 3 AU; spray voltage, 3.50 kV; heater temperature, 438 °C; ion transfer capillary temperature, 320 °C; and S-lens RF level, 50.0. Mass spectrometry was performed using full scan (FS) data and subsequent data-dependent acquisition (DDA). The settings for FS data acquisition were as follows: resolution, 35,000 at *m*/*z* 200; microscans, 1; automatic gain control (AGC) target, 1×10^6; maximum injection time, 120 ms; and scan range, *m*/*z* 50–750. The settings for the DDA mode were as follows: dynamic exclusion, not used; resolution, 17,500 at *m*/*z* 200; microscans, 1; loop count, 5; AGC target, 2×10^4; maximum injection time, 250 ms; isolation window, *m*/*z* 1.0; high collision dissociation (HCD) with stepped normalized collision energy (NCE), 17.5, 35, and 52.5; spectrum data type, profile; and underfill ratio, 1%. TF Xcalibur Qual Browser software version 3.0.63 was used for data handling.

2.3. In Vivo Toxicometabolomics Using ZFL

2.3.1. ZF Husbandry

ZF husbandry and all experiments with ZFL were executed according to EU Directive 2010/63/EU and the German Animal Welfare Act (§11 Abs. 1 TierSchG), in which all works were accomplished by following internal standard operating procedures (SOPs) based on published standard methods. Adult ZF were kept in an automated aquatic ecosystem

(PENTAIR, Apopka, FL, USA), which is a continuous and real-time monitoring system under the following conditions: temperature (27 ± 0.5 °C), pH (7.0 ± 0.1), conductivity (800 ± 50 µS), and light–dark cycle (14 h/10 h). Fish were fed twice a day with dry, small granulate food and freshly hatched live Artemia cysts once per day. The ZFL medium (0.3 × Danieau's solution) was composed of 17 mM NaCl, 2 mM KCl, 0.12 mM $MgSO_4$, 1.8 mM $Ca(NO_3)_2$, 1.5 mM HEPES, pH 7.1–7.3, and 1.2 µM methylene blue. To reproduce ZFL, the ZF pairs were kept overnight in standard mating cages, separated by gender. The following morning, the adult ZF started spawning as soon as the separators were removed. All fertilized eggs of ZF were collected and sorted using a Zeiss Stemi 508 stereo microscope (Carl Zeiss Microscopy GmbH, Jena, Germany). Experiments were carried out with wild-type AB embryos within the first 120 h post fertilization (hpf) as these early life stages are not considered as animal experiments according to the EU Directive 2010/63/EU. At a maximum of 120 hpf, embryos were euthanized by submersion in ice water. All ZFL were raised in an incubator at 28 °C, with a daily medium change to clean the ZFL cultures. The ZFL at 4 dpf were used for drug metabolism studies.

2.3.2. Maximum Tolerated Concentration (MTC) Determination and Bioavailability Estimation

Each compound was treated with 10 ZFL (4 dpf) at 50, 100, and 500 µM concentrations. Naloxone at 300 µM was also done as a treatment as a positive control. Naloxone is known to be tolerated by ZFL upon medium treatment at 300 µM, and its spatial distribution within ZFL has also been studied to validate its bioavailability [19]. This makes it a suitable candidate to be used as a positive control to validate sample preparation steps (described below). Treatment solution contained the compound in 0.3× Danieau's solution with a maximum of 1% DMSO. Treatment was done in a 24-well plate with 1 mL solutions. The ZFL were incubated at 28 °C for 24 h and observed for deaths, malformations, or any visible phenotypic changes under a Zeiss Stemi 508 stereo microscope. The maximum tolerated concentration among the treated concentrations was identified and the ZFL at this concentration were pooled for estimating bioavailability.

For the extraction, the ZFL were washed with 0.3× Danieau's and transferred to an Eppendorf tube. Excess medium was removed using a pipette, the ZFL snap-frozen, and lyophilized for at least 4 h. A volume of 80 µL methanol was then added and the tube was vigorously vortexed for 2 min, followed by centrifugation at 15,000× *g* for 15 min. The supernatant was transferred to a new Eppendorf tube and then sampled for LC-HRMS/MS analysis. All supernatant was transferred to an autosampler vial and 5 µL was injected onto the LC-HRMS/MS system consisting of a Dionex Ultimate 3000 RSLC system (Thermo Fisher Scientific, Germering, Germany) coupled to a maXis 4G HR-QTOF mass spectrometer (Bruker Daltonics, Bremen, Germany) with an Apollo II ESI source. Separation was carried out on a Waters ACQUITY BEH C_{18} column (100 × 2.1 mm, 1.7 µm) equipped with a Waters VanGuard BEH C_{18} 1.7 µm guard column at 45 °C using 0.1% formic acid in water (*v*/*v*, eluent A) and 0.1% formic acid in acetonitrile (*v*/*v*, eluent B) at a flow rate of 600 µL/min. The linear gradient mode was as follows; 0–0.5 min, 5% eluent B; 0.5–18.5 min, 5–95% eluent B; 18.5–20.5 min, 95% eluent B; 20.5–21 min, 95–5% eluent B; and 21–22.5 min, 5% eluent B. A 5 µM pure compound solution in methanol was also run to gauge the ionization behavior of the pure compound.

2.3.3. Experimental Setup for Identification of Metabolites

For each compound, 20 ZFL at 4 dpf were incubated with 3 mL of 100 µM compound solution in a six-well plate. Three such treatments were done in parallel, to have three biological replicates. The solutions were prepared in 0.3× Danieau's with 1% DMSO, which was used as a control incubation with ZFL. The experiment was performed in triplicates.

After 24 h incubation, the ZFL were extracted with the same procedure described above and measured on a TF Q Exactive Plus coupled to a Dionex Ultimate 3000 LC system using data dependent acquisition (DDA) mode with an inclusion list of potential metabolites. The conditions used are summarized under Section 2.2. The inclusion lists used are given in the Supplementary Materials.

Three samples were analyzed in triplicates for each compound—ZF extract and surrounding medium each after 24 h of incubation, and a pure compound solution (100 µM) in 0.3× Danieau's as a control for spontaneous conversion into metabolites upon solvation. Fragment annotation of metabolites was done by comparing their MS^2 spectra with those of the parent compounds using TF XCalibur software. Mass accuracy tolerance of 5 ppm was generally used for characteristic fragment matching, increasing to 10 ppm for low-mass fragments (<100 m/z).

All metabolites detected can only be described as tentatively identified based on their MS^2 spectra, and synthesized authentic standards are required to fully validate and confirm the presence of these compounds. Also, absolute quantification was not performed due to the lack of reference standards for novel metabolites. Relative abundances were assessed semi-quantitatively based on peak area integration to identify major metabolic pathways (see Figures S2 and S3).

2.3.4. Experimental Setup and Analysis Method for Untargeted Metabolomics

For each compound, 20 ZFL at 4 dpf were incubated with 3 mL of 100 µM compound solution in a 6-well plate. The solutions were prepared in 0.3× Danieau's with 1% DMSO, which was used as a control incubation with ZFL. The experiment was performed in triplicates. After 24 h incubation, the ZFL were extracted with the same procedure described above and analyzed on a TF Orbitrap Q Exactive Plus coupled to a Dionex Ultimate 3000 LC system. The elution conditions for reverse phase chromatography were the same as detailed in Section 2.2. HILIC elution was applied using a Merck (Darmstadt, Germany) SeQuant ZIC HILIC (150 mm × 2.1 mm, 3.5 µm). The gradient elution for HILIC was performed using aqueous ammonium acetate (200 mM, eluent C) and acetonitrile containing formic acid (0.1%, v/v, eluent D). The flow rate was set to 500 µL/min using the following gradient: 0–1 min hold 2% C, 1–5 min to 20% C, 5–8.5 min to 60% C, 8.5–10 min hold 60% C, and 10–12 min hold 2% C. The HESI-II source conditions were as follows: ionization mode, positive; sheath gas, 53 AU; auxiliary gas, 14 AU; sweep gas, 3 AU; spray voltage, 3.50 kV; heater temperature, 438 °C; ion transfer capillary temperature, 320 °C; and S-lens RF level, 50.0. Mass spectrometry was performed using full scan (FS) data and subsequent data-dependent acquisition (DDA). The settings for FS data acquisition were as follows: resolution, 140,000 at m/z 200; microscans, 1; automatic gain control (AGC) target, 5×10^5; maximum injection time, 120 ms; and scan range, m/z 50–750. The settings for the DDA mode were as follows: dynamic exclusion, not used; resolution, 35,000 at m/z 200; microscans, 1; loop count, 5; AGC target, 2×10^5; maximum injection time, 100 ms; isolation window, m/z 1.0; high collision dissociation (HCD) with stepped normalized collision energy (NCE), 10, 20, and 40; spectrum data type, profile; and underfill ratio, 1%.

Feature detection was done using TF Compound Discoverer 3.2 (Thermo Fisher Scientific, Waltham, MA, USA) with a predefined untargeted metabolomics workflow—'Untargeted Metabolomics with Statistics Detect Unknowns with ID Using Online Databases and mzLogic'. Among the features observed, the parent compound and its metabolites were also present, and the boundary of p-value for the selection of significant features was set as the highest p-value observed among the parent compound and two of its most abundant metabolites. This resulted in the p-value boundary conditions of 0.004 for DMT-E and 0.006 for DMT-M. Fold change > 2 was used as the fold change criteria. Principal component analysis (PCA) was

used as a further tool to inspect the grouping of significant features. Features with biological group Coefficient of Variance (CV) < 40 in both groups (control and sample) were excluded. Minimum QC coverage of 50% and maximum allowed relative standard deviation of 30% for areas across QC samples were used to exclude features based on QC.

A DDA run was then performed with an inclusion list containing the identified significant features to obtain their MS^2 spectra. Profile data was converted into centroid data using MSConvert 3.0 [39]. Mzmine 4.0 [40] was used to load HMDB [41] and NIST 23 Mass Spectral Library for the MS^2 annotation of significant features with the following settings—scans for matching: MS^2 (all scans); precursor and fragment m/z tolerance: 5 ppm; minimum matched signals: 4; and minimum cosine similarity: 0.7 (without precursor).

3. Results

3.1. In Vitro Metabolism Using pHLS9 Fraction

The proposed metabolic pathways for the two compounds in pHLS9 (and ZFL) are shown in Figure 2. DMT-E metabolic steps included *N*-demethylation and the hydroxylation of the alkyl chain. A total of three in vitro metabolites were observed for DMT-M and included *N*-demethylation, as well as alkyl chain hydroxylation and *N*-oxide formation. Key fragments used to annotate the metabolites are discussed in the later section. The above-described metabolites were detected in incubations containing pHLS9, as well as in low amounts (<10 fold) in neat samples and control samples without pHLS9, suggesting the occurrence of spontaneous conversion into metabolites to an extent upon solvation. Other potential reasons for the occurrence of metabolites in neat/control samples could be due to synthesis byproducts, build-up over storage, or HRMS artifacts. However, since the peak areas increased over time in pHLS9 incubations, their formation was concluded to also be results of enzymatic activity. Neither of the compounds were metabolized to DMT at least in detectable amounts. Nevertheless, certain amounts of DMT (near 1/6th of pure compound for DMT-M, and near 1/500th for DMT-E, based on peak areas) were already present in both stock solutions and areas did not increase after incubations.

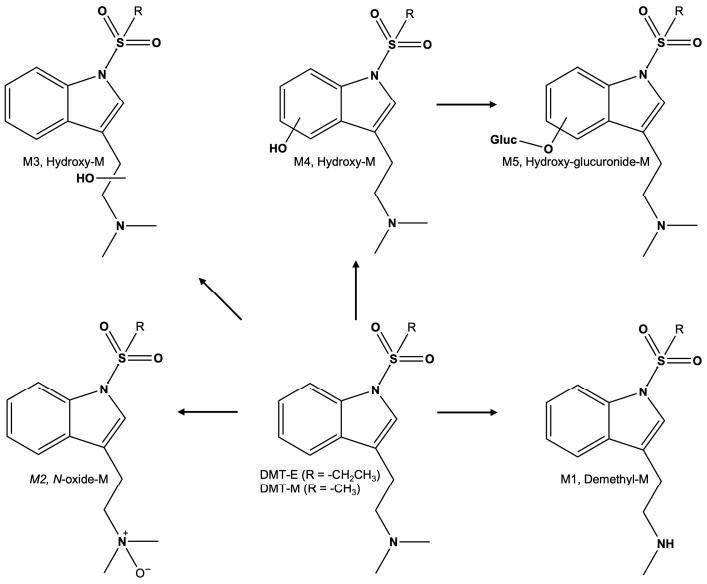

Figure 2. Proposed metabolic pathways for *N*,*N*-dimethyltryptamine esylate (DMT-E) and *N*,*N*-dimethyltryptamine mesylate (DMT-M) based on combined results from both ZFL and pHLS9. (R = $-CH_2CH_3$ or $-CH_3$), M = metabolite.

3.2. MTC and Bioavailability in ZFL

Among the three tested concentrations, 50 and 100 µM concentrations caused no visible morphological changes such as twisted tail or development of an edema (Table 1). However, at the 500 µM concentration, lethality was observed in both compound treatments. Therefore, 100 µM was fixed as the treatment concentration for all studies.

Table 1. Results of the maximum tolerated concentration (MTC) tests. Observations were made visually after 24 h incubation under a microscope by comparison with untreated larvae.

Compound	Concentrations Tested, µM	MTC and Survival Rate	Notable Observations
DMT-E	50, 100, 500	100 µM, 10/10	100% lethality and twisted tail at 500 µM
DMT-M	50, 100, 500	100 µM, 10/10	Slow movement at 100 µM 20% lethality at 500µM

Results from the bioavailability estimation experiments are shown in Figure 3. Both compounds were detected at high intensities (compared to a 5 µM pure compound solution) in the ZFL extract after treatment at their MTC, suggesting favorable oral bioavailability and ionization behavior. The ratio of intensities between ZFL extract and pure compound solution was seen to be much higher in the case of both compounds as compared to Naloxone, which is a compound known to be bioavailable from previous studies [19].

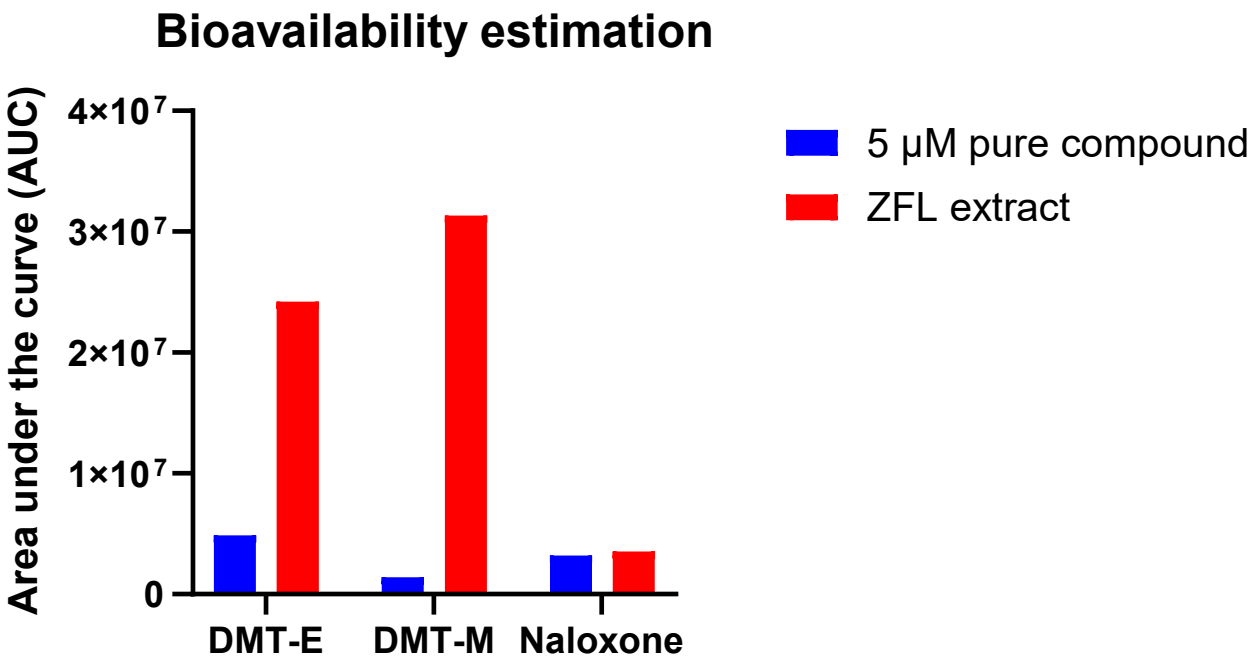

Figure 3. Graph comparing intensities of $M+H^+$ of the compounds in ZFL extract at MTC. In total, 5 µM pure compound in methanol was analyzed as an indicator of ease of ionization.

3.3. In Vivo Metabolism Using ZFL

The proposed metabolic pathways for the two compounds in ZFL (and pHLS9) are shown in Figure 2. The peak areas, retention times, and calculated elemental compositions of the proposed molecules are shown in the Supporting Information (Tables S1 and S2). The MS^2 spectra for DMT-E metabolites are exemplified in Figure 4. The data for DMT-M metabolites are shown in the Supplementary Materials (Table S2).

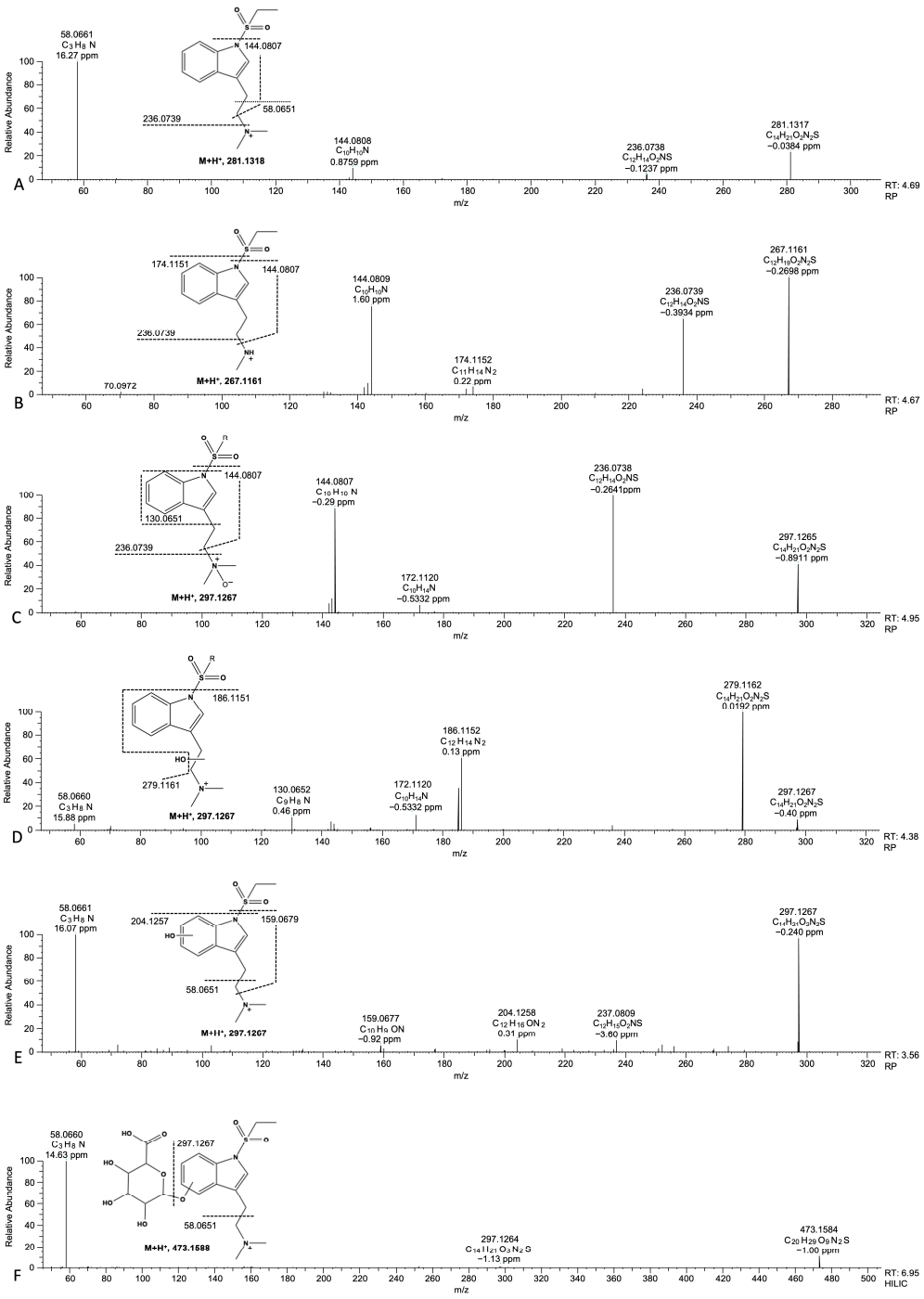

Figure 4. MS^2 spectra and fragment annotations for *N*,*N*-dimethyltryptamine esylate (**A**) and its metabolites (**B**–**F**) resulting from demethylation (**B**), *N*-oxidation (**C**), aliphatic hydroxylation (**D**), aromatic hydroxylation (**E**), and aromatic hydroxylation + glucuronidation (**F**). The spectra were derived at the retention time of highest intensity (detailed in the Supplementary Materials) and remained consistent across replicates.

In total, four phase I and one phase II metabolite could be found in ZFL. Hydroxylation and demethylation resulted in metabolites with high relative intensities, and glucuronidation after hydroxylation was identified as the only phase II metabolite. As was the case for pHLS9 incubations, some metabolites could be detected in low amounts in neat samples and control samples (Figures S2, S3, S6 and S7), suggesting the occurrence of spontaneous conversion into metabolites to an extent upon solvation. As mentioned in Section 3.1, other potential reasons for the occurrence of some metabolites in neat/control samples could be

due to synthesis byproducts, build-up over storage, or HRMS artifacts. However, since the peak areas increased over time in ZFL incubations, their formation was concluded to also be results of enzymatic activity.

In both parent compounds (DMT-E and DMT-M), cleavage of the C-C bond resulted in a fragment corresponding to an iminium cation (m/z = 58.0651) that was seen in high relative intensities in accordance with reported spectra from DMT and many of its derivatives (available on NIST 23 mass spectral database). This cleavage resulted in a stable *N* cation and a resonance stabilized counter ion, explaining the favorable formation. The lack of this peak at high intensity indicated *N*-demethylation, and/or hydroxylation that prevents the formation of this fragment ion.

3.4. Untargeted Toxicometabolomics Using ZFL

Nine upregulated features and one downregulated feature were observed upon ZFL DMT-E exposure. The m/z and putative classifications of the compounds are given in the Supplementary Materials, along with principal component analysis (PCA) plots and volcano plots. The upregulated features mostly consist of the parent compound and its metabolites. The only endogenous compound that was well annotated was *L*-threonine (or one of its closely related isomers), which was observed to be downregulated. The MS^2 spectrum is shown in Figure 5.

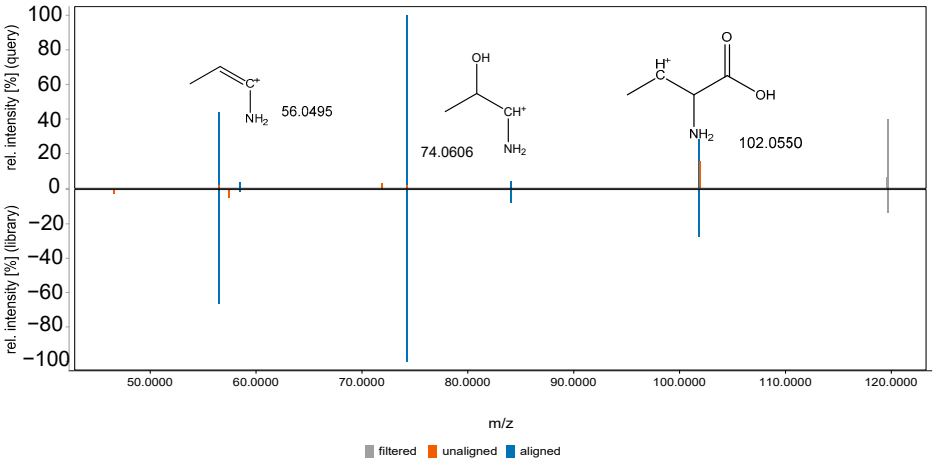

Figure 5. MS^2 spectrum and identification of downregulated feature as L-threonine (m/z = 120.0665). Library—Human Metabolome Database (HMDB) [32]. Cosine score = 0.880. EntryID—HMDB0000167.

ZFL DMT-M treatment resulted in 15 significant features, of which most were upregulated. Most of the upregulated features were once again identified to be the metabolites of the parent compound and the remaining few could not be identified yet. Threonine was once again identified as a downregulated feature.

4. Discussion

4.1. In Vitro Metabolism Using pHLS9 Fraction

Incubation with pHLS9 fraction resulted in phase I metabolites, with hydroxylation and demethylation being the most favored pathways. Conjugation with glucuronide or sulfate could not be detected for any of the investigated substances, suggesting the lack of phase II metabolism. This contrasts with what was observed in the ZFL system (as discussed later), where a metabolite formed after glucuronidation was observed. The absence of this metabolite, and a relatively lower overall number of metabolites in the pHLS9 system as compared to the ZFL system is in line with the observations from previous studies [16].

4.2. MTC and Bioavailability in ZFL

Given the lack of any lethality or morphological effects, 100 µM was an easy choice for subsequent treatments, although it is likely that there is a concentration between 100 and 500 µM, which is also well tolerated, further treatment concentrations were not tested given the observation of a favorable bioavailability even at 100 µM, as discussed below. Upon DMT-M treatment, ZFL were observed to move slower as compared to untreated larvae, while DMT-E treatment did not induce such an effect, suggesting a difference in the pathways being affected upon uptake.

In the bioavailability study, the ratio of intensities between ZFL extract and pure compound solution was seen to be much higher in the case of both compounds as compared to naloxone, which is a compound known to be bioavailable from previous studies [19]. Although more robust analyses are required to quantitatively compare bioavailability across compounds, the graph nonetheless suggests a very favorable bioavailability for the two compounds, preventing the need to perform a microinjection for treatment. This can be justified by the lack of free charges, and that the compounds contain almost no hydrogen bond donors or acceptors [42]. Moreover, they are small molecules which makes them more likely to penetrate membranes.

4.3. In Vivo Metabolism Using ZFL

All metabolic transformations observed in pHLS9 incubations were also detected in the ZFL extracts, along with additional transformations such as glucuronidation. HPLC chromatograms (depicted in the Supplementary Materials) clearly suggest that there are multiple isomers generated via hydroxylation and glucuronidation pathways, some of which have not been described due to the lack of reliable MS^2 structure elucidation for those isomers. The total number of metabolites detected is understandably higher in ZFL extracts as compared to pHLS9 incubations, since such a difference due to the model systems was also reported for other psychoactive compounds in the past [16], and highlights the value of ZFL as a model to predict metabolism.

The most abundant metabolite observed was the *N*-oxide following a hydroxylation at the tertiary amine. Although *N*-oxide formation was observed in controls, the abundance after ZFL exposure was > 10-fold higher, confirming a relevant enzymatic contribution (shown in detail in the Supplementary Materials). All other metabolites were observed in relatively high amounts in the ZFL extracts, suggesting that they were metabolized by the ZFL. Most of the phase I metabolites detected are expected to have been generated by Cytochrome P450 (CYP) enzymes [43], and ZFL are known to possess orthologs of human CYP enzymes [44]. It was observed in the case of DMT (and other tryptamines such as 5-MeO-DMT) that CYP2D6 was the main CYP enzyme responsible for its metabolism [45–47], but studies investigating the enzymes responsible for metabolizing sulfonated tryptamines are lacking. Given that sulfonated tryptamines are known to have deviating enzymatic preferences compared to DMT, which is reflected in their ability to bind to the $5HT_6$ receptor instead of $5HT_2A$ [30,31], it is possible that they are metabolized by a different set of CYP enzymes. In vitro inhibition studies and phenotypic screens have been described for tryptamines [45,46], and similar approaches can be applied to investigate the key enzymes involved in metabolizing the compounds in this study.

Conversion of the tertiary amine into an acetic acid moiety was not observed for either of the compounds, which is rather interesting given that indole acetic acid (IAA) is the primary metabolite of DMT [48]. The conversion of DMT into IAA is performed by monoamine oxidase (MAO) enzymes rapidly upon uptake, which hinders the therapeutic potential of DMT [22]. Although studies exploring DMT metabolism in zebrafish are lacking, the existence of a functionally active MAO in zebrafish has been well documented,

and the principal characterizing domains are known to be conserved [49]. The lack of conversion of the compounds into IAA suggests that MAO is inactive on the compounds, thereby suggesting the absence of the kind of first pass metabolism known to be an issue in the case of DMT. The inactivity of MAO on the compound would explain the lack of formation of the IAA metabolite, thus leading to the preferential formation of hydroxylated and demethylated metabolites as the main phase I metabolites. However, neither of the compounds went through a conversion into DMT, which hampers the therapeutic potential of the compounds in their use as DMT prodrugs.

The metabolism observed for the DMT-M derivative (see Table S2 in the Supplementary Materials) closely resembles what was also observed for DMT-E, which suggests that the presence of an additional methyl group does not affect the binding of the molecule to its metabolizing enzymes. Given the structural similarity, it is understandable that both derivatives undergo similar biotransformation. Although difficult to predict, it is also possible that some of the metabolites retain a therapeutic potential, either by 5-HT_6 binding like the parent compound, or by other unexplored mechanisms. The main binding moiety for the 5-HT_6 receptor, in the case of sulfonyl tryptamines, is a protonated amine [50], which was not significantly altered in most of the biotransformations observed. Further studies are necessary to investigate if the observed metabolites retain binding ability and therapeutic potential.

4.4. Untargeted Toxicometabolomics Using ZFL

Untargeted toxicometabolomics studies allow the detection and identification of endogenous and exogenous biomarkers after drug exposure. This enables the determination of metabolites (as discussed in the previous section) of the investigated substance in order to detect an intake by patients, as well as the identification of biomarkers that provide information on the (off target) effects in only one experiment [51,52].

Threonine is an essential amino acid that is known to play a key role in diverse physiological processes including protein synthesis, lipid metabolism, embryonic stem cell differentiation, and intestinal gut health regulation [53]. The downregulation of threonine could occur because of increased synthesis of threonine-rich proteins, or because of reduced biosynthesis, or due to a more complicated mechanism that requires further investigation.

Threonine was identified as a downregulated feature in both compound treatments, suggesting that the two derivatives have a similar mode of action. Interestingly, ayahuasca—the natural DMT-containing substance through which DMT is widely consumed, is known to alter the levels of large neutral amino acids, but not threonine [54].

5. Conclusions

This study offers valuable insights into the biotransformation and metabolomic response following treatment with two novel sulfonated derivatives of DMT, utilizing pHLS9 and ZFL as model systems. For each compound, five phase I and one phase II metabolite was identified in ZFL, while fewer phase I metabolites were detected after pHLS9 incubation. The two main metabolic reactions were identified to be hydroxylation and demethylation. Glucuronidation upon hydroxylation on the ring was the only phase II reaction observed. Notably, the generation of an acetic acid moiety—a major biotransformation pathway for DMT and a key limitation to its therapeutic use—was absent. The loss of the sulfonation to yield DMT was also not observed neither in pHLS9 nor on ZFL, suggesting that sulfonation does not act as a prodrug mechanism for the compounds in these model systems. Further investigation using advanced metabolism models, including human microdosing, is warranted to elucidate this mechanism. However, these spectral

data provide the necessary foundation for forensic laboratories and doping laboratories to identify these NPS in biological samples.

Threonine was the only identified endogenous metabolite to be significantly altered upon treatment with both compounds. Some significant features were identified as metabolites of the parent compound supporting prior observations from the targeted approach, but several remain unidentified due to the limited availability of a dedicated ZFL metabolite library. Identification of endogenous ZFL metabolites is a challenge given the lack of an existing library specifically containing ZFL metabolites. Moreover, the lack of more endogenous biomarkers suggests a possible scope in further optimization of sample preparation steps such as ZFL pool size, extraction and injection volumes, etc. Nevertheless, the metabolites and biomarkers identified in this study can be used in a targeted approach to analyze intake of these synthetic tryptamine derivatives. Overall, this study advances the understanding of synthetic tryptamine metabolism and their effects on the metabolome. Nonetheless, further research is essential to validate these findings and assess their relevance to human physiology.

Supplementary Materials: The following supporting information can be downloaded at: https://www.mdpi.com/article/10.3390/metabo16020134/s1, Figure S1. Timeline and steps of preparation of Zebrafish Larvae (ZFL) for metabolism and untargeted metabolomics studies. Health checks are performed visually using a simple microscope; Table S1. Retention time (apex) and m/z values for metabolites (structures given in main manuscript) observed for DMT-E. All molecules were detected as ions in their protonated form in positive mode using a reversed-phase column (see experimental section of main manuscript); Table S2. Retention time (apex) and m/z values for metabolites (structures given in main manuscript) observed for DMT-M. All molecules were detected as ions in their protonated form in positive mode using a reversed-phase column (see experimental section of main manuscript); Figure S2. Area under the curve for metabolites of DMT-E, as a potential indicator of relative abundance. SM = Surrounding medium collected after 1 day incubation with Zebrafish Larvae (ZFL); Figure S3. Area under the curve for metabolites of DMT-M, as a potential indicator of relative abundance. SM = Surrounding medium collected after 1 day incubation with Zebrafish Larvae (ZFL); Figure S4. Principal component analysis (PCA) plots from untargeted metabolomics studies of DMT-E and DMT-M respectively; Figure S5. Volcano plots from untargeted metabolomics studies with DMT-E and DMT-M respectively. Fold change > 2 was used as the fold change criteria and p-value boundary was set as 0.004 for DMT-E and 0.006 for DMT-M. Red shaded area covers upregulated features, and green shaded area covers downregulated features; Table S3. Overview of significant features detected upon DMT-E treatment using Compound Discoverer. All features were detected using a zicHILIC column and in positive polarity. Identities were predicted using retention time (min), m/z, and MS/MS spectra using mzMine. MSI level = level of identification according to Metabolomics Standards Initiative (MSI); Figure S6. Extracted Ion Chromatograms corresponding to DMT-E and its metabolites; Figure S7. Extracted Ion Chromatograms corresponding to DMT-E and its metabolites; Figure S8. Overlay of total ion chromatograms (TIC) of pure compound (100 µM) in ZFL Incubation medium and medium blank solution; Table S4. Overview of significant features detected upon DMT-M treatment using Compound Discoverer. All features were detected using a zicHILIC column and in positive polarity. Identities were predicted using retention time (min), m/z, and MS/MS spectra using mzMine. MSI level = level of identification according to Metabolomics Standards Initiative (MSI) [55]; Table S5. Inclusion lists used for the metabolism study of DMT-E and DMT-M, respectively, for reliable generation of MS/MS data through data-dependent acquisition (DDA). S.No = Serial number; Table S6. Inclusion list used for the second run of untargeted metabolomics study for reliable generation of MS/MS data of significant features; Schematic S1. Chemical Synthesis of DMT-E; Schematic S2. Chemical Synthesis of DMT-M.

Author Contributions: Conceptualization, P.P., J.H. and M.R.M.; methodology, P.P., S.K.M., S.H., P.S., J.H. and M.R.M.; formal analysis, P.P., S.K.M. and S.H.; investigation, P.P., S.K.M., S.H., P.S., J.H. and M.R.M.; resources, J.H., M.G. and M.R.M.; data curation, P.P., S.K.M., S.H. and P.S.; writing—original draft preparation, P.P.; writing—review and editing, P.P., S.K.M., S.H., P.S., M.G., J.H. and M.R.M.; visualization, P.P. and S.H.; supervision, J.H. and M.R.M.; project administration, J.H. and M.R.M. All authors have read and agreed to the published version of the manuscript.

Funding: This research was funded by Saarland University, the TALENTS Marie Skłodowska-Curie COFUND-Action of the European Union [101081463], received by LAGM.

Institutional Review Board Statement: Not applicable.

Informed Consent Statement: Not applicable.

Data Availability Statement: Further data is available from the corresponding author upon reasonable request.

Acknowledgments: The authors would like to thank Andreas Kany, Sari Rasheed, F.P. Jake Haeckl, Felix Deschner, Franziska Fries and Timo Risch for their support and/or helpful discussion.

Conflicts of Interest: Author Matthias Grill was employed by the company MIKHAL. The remaining authors declare that the research was conducted in the absence of any commercial or financial relationships that could be construed as a potential conflict of interest.

Abbreviations

The following abbreviations are used in this manuscript:

NPS	Novel psychoactive substances
EMCDDA	European Monitoring Centre for Drugs and Drug Addiction
ZF	Zebrafish
ZFL	Zebrafish larvae
dpf	Days post fertilization
DMT	*N*,*N*-dimethyltryptamine
MAO-A	Monoamine oxidase-A
DMT-E	DMT esylate
DMT-M	DMT mesylate
DMSO	Dimethyl sulfoxide
PAPS	3′-Phosphoadenosine-5′-phosphosulfate
SAM	S-(5′-Adenosyl)-l-methionine
DTT	Dithiothreitol
GSH	Reduced glutathione
AcT	Acetylcarnitine transferase
AcCoA	Acetyl coenzyme A
pHLS9	Pooled human liver S9 fraction
LC-HR-MS/MS	Liquid chromatography–high-resolution mass spectrometry
AGC	Automatic gain control
NCE	Normalized collision energy
SOPs	Standard operating procedures
MTC	Maximum tolerated concentration
DDA	Data dependent acquisition
HCD	High collision dissociation
PCA	Principal component analysis

References

1. European Union Drugs Agency (EUDA). *European Drug Report 2024: Trends and Developments*; European Union Drugs Agency (EUDA): Lisbon, Portugal, 2024.

2. Maurer, H.H.; Pfleger, K.; Weber, A.A. *Mass Spectral Data of Drugs, Poisons, Pesticides, Pollutants and Their Metabolites*; Wiley-VCH: Weinheim, Germany, 2016.
3. Manier, S.K.; Keller, A.; Schaper, J.; Meyer, M.R. Untargeted metabolomics by high resolution mass spectrometry coupled to normal and reversed phase liquid chromatography as a tool to study the in vitro biotransformation of new psychoactive substances. *Sci. Rep.* **2019**, *9*, 2741. [CrossRef]
4. Araujo, A.M.; Carvalho, M.; Costa, V.M.; Duarte, J.A.; Dinis-Oliveira, R.J.; Bastos, M.L.; Guedes de Pinho, P.; Carvalho, F. In vivo toxicometabolomics reveals multi-organ and urine metabolic changes in mice upon acute exposure to human-relevant doses of 3,4-methylenedioxypyrovalerone (MDPV). *Arch. Toxicol.* **2021**, *95*, 509–527. [CrossRef] [PubMed]
5. Steuer, A.E.; Kaelin, D.; Boxler, M.I.; Eisenbeiss, L.; Holze, F.; Vizeli, P.; Czerwinska, J.; Dargan, P.I.; Abbate, V.; Liechti, M.E.; et al. Comparative Untargeted Metabolomics Analysis of the Psychostimulants 3,4-Methylenedioxy-Methamphetamine (MDMA), Amphetamine, and the Novel Psychoactive Substance Mephedrone after Controlled Drug Administration to Humans. *Metabolites* **2020**, *10*, 306. [CrossRef]
6. Manier, S.K.; Schwermer, F.; Wagmann, L.; Eckstein, N.; Meyer, M.R. Liquid Chromatography-High-Resolution Mass Spectrometry-Based In Vitro Toxicometabolomics of the Synthetic Cathinones 4-MPD and 4-MEAP in Pooled Human Liver Microsomes. *Metabolites* **2020**, *11*, 3. [CrossRef]
7. Hemmer, S.; Wagmann, L.; Meyer, M.R. Altered metabolic pathways elucidated via untargeted in vivo toxicometabolomics in rat urine and plasma samples collected after controlled application of a human equivalent amphetamine dose. *Arch. Toxicol.* **2021**, *95*, 3223–3234. [CrossRef]
8. Zaitsu, K.; Hayashi, Y.; Kusano, M.; Tsuchihashi, H.; Ishii, A. Application of metabolomics to toxicology of drugs of abuse: A mini review of metabolomics approach to acute and chronic toxicity studies. *Drug Metab. Pharmacokinet.* **2016**, *31*, 21–26. [CrossRef]
9. Hemmer, S.; Manier, S.K.; Wagmann, L.; Meyer, M.R. Comparison of reversed-phase, hydrophilic interaction, and porous graphitic carbon chromatography columns for an untargeted toxicometabolomics study in pooled human liver microsomes, rat urine, and rat plasma. *Metabolomics* **2024**, *20*, 49. [CrossRef]
10. Hemmer, S.; Wagmann, L.; Pulver, B.; Westphal, F.; Meyer, M.R. In Vitro and In Vivo Toxicometabolomics of the Synthetic Cathinone PCYP Studied by Means of LC-HRMS/MS. *Metabolites* **2022**, *12*, 1209. [CrossRef] [PubMed]
11. Abraham, A.; Wang, Y.; El Said, K.R.; Plakas, S.M. Characterization of brevetoxin metabolism in Karenia brevis bloom-exposed clams (*Mercenaria* sp.) by LC-MS/MS. *Toxicon* **2012**, *60*, 1030–1040. [CrossRef] [PubMed]
12. Wang, L.; Wu, N.; Zhao, T.Y.; Li, J. The potential biomarkers of drug addiction: Proteomic and metabolomics challenges. *Biomarkers* **2016**, *21*, 678–685. [CrossRef]
13. Steuer, A.E.; Brockbals, L.; Kraemer, T. Metabolomic Strategies in Biomarker Research-New Approach for Indirect Identification of Drug Consumption and Sample Manipulation in Clinical and Forensic Toxicology? *Front. Chem.* **2019**, *7*, 319. [CrossRef]
14. Choi, T.Y.; Choi, T.I.; Lee, Y.R.; Choe, S.K.; Kim, C.H. Zebrafish as an animal model for biomedical research. *Exp. Mol. Med.* **2021**, *53*, 310–317. [CrossRef] [PubMed]
15. Alseekh, S.; Aharoni, A.; Brotman, Y.; Contrepois, K.; D'auria, J.; Ewald, J.; Ewald, J.C.; Fraser, P.D.; Giavalisco, P.; Hall, R.D.; et al. Mass spectrometry-based metabolomics: A guide for annotation, quantification and best reporting practices. *Nat. Methods* **2021**, *18*, 747–756. [CrossRef]
16. RRichter, L.H.; Herrmann, J.; Andreas, A.; Park, Y.M.; Wagmann, L.; Flockerzi, V.; Müller, R.; Meyer, M.R. Tools for studying the metabolism of new psychoactive substances for toxicological screening purposes—A comparative study using pooled human liver S9, HepaRG cells, and zebrafish larvae. *Toxicol. Lett.* **2019**, *305*, 73–80. [CrossRef] [PubMed]
17. Cooman, T.; Hoover, B.; Sauvé, B.; Bergeron, S.A.; Quinete, N.; Gardinali, P.; Arroyo, L.E. The metabolism of valerylfentanyl using human liver microsomes and zebrafish larvae. *Drug Test. Anal.* **2022**, *14*, 1116–1129. [CrossRef] [PubMed]
18. Park, Y.M.; Meyer, M.R.; Müller, R.; Herrmann, J. Drug Administration Routes Impact the Metabolism of a Synthetic Cannabinoid in the Zebrafish Larvae Model. *Molecules* **2020**, *25*, 4474. [CrossRef]
19. Park, Y.M.; Meyer, M.R.; Müller, R.; Herrmann, J. Optimization of Mass Spectrometry Imaging for Drug Metabolism and Distribution Studies in the Zebrafish Larvae Model: A Case Study with the Opioid Antagonist Naloxone. *Int. J. Mol. Sci.* **2023**, *24*, 10076. [CrossRef]
20. Schippers, P.; Rasheed, S.; Park, Y.M.; Risch, T.; Wagmann, L.; Hemmer, S.; Manier, S.K.; Müller, R.; Herrmann, J.; Meyer, M.R. Evaluation of extraction methods for untargeted metabolomic studies for future applications in zebrafish larvae infection models. *Sci. Rep.* **2023**, *13*, 7489. [CrossRef]
21. Barker, S.A.; Monti, J.A.; Christian, S.T. N,N-Dimethyltryptamine: An Endogenous Hallucinogen. In *International Review of Neurobiology*; Smythies, J.R., Bradley, R.J., Eds.; Academic Press: Cambridge, MA, USA, 1981; Volume 22, pp. 83–110.
22. Rodrigues, A.V.; Almeida, F.J.; Vieira-Coelho, M.A. Dimethyltryptamine: Endogenous Role and Therapeutic Potential. *J. Psychoact. Drugs* **2019**, *51*, 299–310. [CrossRef]
23. Carbonaro, T.M.; Gatch, M.B. Neuropharmacology of N,N-dimethyltryptamine. *Brain Res. Bull.* **2016**, *126*, 74–88. [CrossRef]

24. Agurell, S.; Holmstedt, B.; Lindgren, J.E. Metabolism of 5-methoxy-N,N dimethyltryptamine-14C in the rat. *Biochem. Pharmacol.* **1969**, *18*, 2771–2781. [CrossRef] [PubMed]
25. Osamu, S.; Katsumata, Y.; Masakazu, O. Characterization of eight biogenic indoleamines as substrates for type A and type B monoamine oxidase. *Biochem. Pharmacol.* **1981**, *30*, 1353–1358. [CrossRef]
26. Egger, K.; Aicher, H.D.; Cumming, P.; Scheidegger, M. Neurobiological research on N,N-dimethyltryptamine (DMT) and its potentiation by monoamine oxidase (MAO) inhibition: From ayahuasca to synthetic combinations of DMT and MAO inhibitors. *Cell. Mol. Life Sci.* **2024**, *81*, 395. [CrossRef]
27. Nyandege, A.; Kolanos, R.; Roth, B.L.; Glennon, R.A. Further studies on the binding of N1-substituted tryptamines at h5-HT6 receptors. *Bioorganic Med. Chem. Lett.* **2007**, *17*, 1691–1694. [CrossRef]
28. Kalgutkar, A.; Jones, R.; Sawant, A. Chapter 5. Sulfonamide as an Essential Functional Group in Drug Design. *RSC Drug Discov. Ser.* **2010**, *1*, 210–274. [CrossRef]
29. Shu, Y.-Z.; Johnson, B.M.; Yang, T.J. Role of Biotransformation Studies in Minimizing Metabolism-Related Liabilities in Drug Discovery. *AAPS J.* **2008**, *10*, 178–192. [CrossRef]
30. Glennon, R.A.; Chaurasia, C.; Titeler, M. Binding of indolylalkylamines at 5-HT2 serotonin receptors: Examination of a hydrophobic binding region. *J. Med. Chem.* **1990**, *33*, 2777–2784. [CrossRef]
31. Almaula, N.; Ebersole, B.J.; Zhang, D.; Weinstein, H.; Sealfon, S.C. Mapping the binding site pocket of the serotonin 5-hydroxytryptamine$_{2A}$ receptor: Ser$^{3.36(159)}$ provides a second interaction Site for the protonated amine of serotonin but not of lysergic acid diethylamide or bufotenin. *J. Biol. Chem.* **1996**, *271*, 14672–14675. [CrossRef]
32. Rosse, G.; Schaffhauser, H. 5-HT6 receptor antagonists as potential therapeutics for cognitive impairment. *Curr. Top. Med. Chem.* **2010**, *10*, 207–221. [CrossRef] [PubMed]
33. Ramírez, M.J. 5-HT6 receptors and Alzheimer's disease. *Alzheimer's Res. Ther.* **2013**, *5*, 15. [CrossRef]
34. Richter, L.H.J.; Flockerzi, V.; Maurer, H.H.; Meyer, M.R. Pooled human liver preparations, HepaRG, or HepG2 cell lines for metabolism studies of new psychoactive substances? A study using MDMA, MDBD, butylone, MDPPP, MDPV, MDPB, 5-MAPB, and 5-API as examples. *J. Pharm. Biomed. Anal.* **2017**, *143*, 32–42. [CrossRef] [PubMed]
35. Richter, L.H.J.; Maurer, H.H.; Meyer, M.R. New psychoactive substances: Studies on the metabolism of XLR-11, AB-PINACA, FUB-PB-22, 4-methoxy-alpha-PVP, 25-I-NBOMe, and meclonazepam using human liver preparations in comparison to primary human hepatocytes, and human urine. *Toxicol. Lett.* **2017**, *280*, 142–150. [CrossRef]
36. Dalvie, D.; Obach, R.S.; Kang, P.; Prakash, C.; Loi, C.M.; Hurst, S.; Nedderman, A.; Goulet, L.; Smith, E.; Bu, H.Z.; et al. Assessment of three human in vitro systems in the generation of major human excretory and circulating metabolites. *Chem. Res. Toxicol.* **2009**, *22*, 357–368. [CrossRef] [PubMed]
37. Caspar, A.T.; Helfer, A.G.; Michely, J.A.; Auwarter, V.; Brandt, S.D.; Meyer, M.R.; Maurer, H.H. Studies on the metabolism and toxicological detection of the new psychoactive designer drug 2-(4-iodo-2,5-dimethoxyphenyl)-N-[(2-methoxyphenyl)methyl]ethanamine (25I-NBOMe) in human and rat urine using GC-MS, LC-MS(n), and LC-HR-MS/MS. *Anal. Bioanal. Chem.* **2015**, *407*, 6697–6719. [CrossRef]
38. Helfer, A.G.; Michely, J.A.; Weber, A.A.; Meyer, M.R.; Maurer, H.H. Orbitrap technology for comprehensive metabolite-based liquid chromatographic-high resolution-tandem mass spectrometric urine drug screening—Exemplified for cardiovascular drugs. *Anal. Chim. Acta* **2015**, *891*, 221–233. [CrossRef]
39. Adusumilli, R.; Mallick, P. Data Conversion with ProteoWizard msConvert. *Methods Mol. Biol.* **2017**, *1550*, 339–368. [CrossRef]
40. Schmid, R.; Heuckeroth, S.; Korf, A.; Smirnov, A.; Myers, O.; Dyrlund, T.S.; Bushuiev, R.; Murray, K.J.; Hoffmann, N.; Lu, M.; et al. Integrative analysis of multimodal mass spectrometry data in MZmine 3. *Nat. Biotechnol.* **2023**, *41*, 447–449. [CrossRef]
41. Wishart, D.S.; Guo, A.; Oler, E.; Wang, F.; Anjum, A.; Peters, H.; Dizon, R.; Sayeeda, Z.; Tian, S.; Lee, B.L.; et al. HMDB 5.0: The Human Metabolome Database for 2022. *Nucleic Acids Res.* **2022**, *50*, D622–D631. [CrossRef]
42. Lipinski, C.A.; Lombardo, F.; Dominy, B.W.; Feeney, P.J. Experimental and computational approaches to estimate solubility and permeability in drug discovery and development settings. *Adv. Drug Deliv. Rev.* **1997**, *23*, 3–25. [CrossRef]
43. Zhao, M.; Ma, J.; Li, M.; Zhang, Y.; Jiang, B.; Zhao, X.; Huai, C.; Shen, L.; Zhang, N.; He, L.; et al. Cytochrome P450 Enzymes and Drug Metabolism in Humans. *Int. J. Mol. Sci.* **2021**, *22*, 12808. [CrossRef]
44. Nawaji, T.; Yamashita, N.; Umeda, H.; Zhang, S.; Mizoguchi, N.; Seki, M.; Kitazawa, T.; Teraoka, H. Cytochrome P450 Expression and Chemical Metabolic Activity before Full Liver Development in Zebrafish. *Pharmaceuticals* **2020**, *13*, 456. [CrossRef]
45. Shen, H.W.; Wu, C.; Jiang, X.L.; Yu, A.M. Effects of monoamine oxidase inhibitor and cytochrome P450 2D6 status on 5-methoxy-N,N-dimethyltryptamine metabolism and pharmacokinetics. *Biochem. Pharmacol.* **2010**, *80*, 122–128. [CrossRef]
46. Good, M.; Joel, Z.; Benway, T.; Routledge, C.; Timmermann, C.; Erritzoe, D.; Weaver, R.; Allen, G.; Hughes, C.; Topping, H.; et al. Pharmacokinetics of N,N-dimethyltryptamine in Humans. *Eur. J. Drug Metab. Pharmacokinet.* **2023**, *48*, 311–327. [CrossRef]
47. Eckernäs, E.; Macan-Schönleben, A.; Andresen-Bergström, M.; Birgersson, S.; Hoffmann, K.-J.; Ashton, M. N,N-dimethyltryptamine forms oxygenated metabolites via CYP2D6—An in vitro investigation. *Xenobiotica* **2023**, *53*, 515–522. [CrossRef]

48. Brito-da-Costa, A.M.; Dias-da-Silva, D.; Gomes, N.G.M.; Dinis-Oliveira, R.J.; Madureira-Carvalho, ü. Toxicokinetics and Toxicodynamics of Ayahuasca Alkaloids N,N-Dimethyltryptamine (DMT), Harmine, Harmaline and Tetrahydroharmine: Clinical and Forensic Impact. *Pharmaceuticals* **2020**, *13*, 334. [CrossRef] [PubMed]
49. Setini, A.; Pierucci, F.; Senatori, O.; Nicotra, A. Molecular characterization of monoamine oxidase in zebrafish (*Danio rerio*). *Comp. Biochem. Physiol. Part B Biochem. Mol. Biol.* **2005**, *140*, 153–161. [CrossRef] [PubMed]
50. Dukat, M.; Mosier, P.D.; Kolanos, R.; Roth, B.L.; Glennon, R.A. Binding of serotonin and N1-benzenesulfonyltryptamine-related analogs at human 5-HT6 serotonin receptors: Receptor modeling studies. *J. Med. Chem.* **2008**, *51*, 603–611. [CrossRef] [PubMed]
51. Bouhifd, M.; Hartung, T.; Hogberg, H.T.; Kleensang, A.; Zhao, L. Review: Toxicometabolomics. *J. Appl. Toxicol.* **2013**, *33*, 1365–1383. [CrossRef]
52. Milburn, M.V.; Ryals, J.A.; Guo, L. Toxicometabolomics. In *A Comprehensive Guide to Toxicology in Nonclinical Drug Development*; Academic Press: Cambridge, MA, USA, 2013; pp. 875–891. [CrossRef]
53. Tang, Q.; Tan, P.; Ma, N.; Ma, X. Physiological Functions of Threonine in Animals: Beyond Nutrition Metabolism. *Nutrients* **2021**, *13*, 2592. [CrossRef]
54. Madrid-Gambin, F.; Gomez-Gomez, A.; Busquets-Garcia, A.; Haro, N.; Marco, S.; Mason, N.L.; Reckweg, J.T.; Mallaroni, P.; Kloft, L.; van Oorsouw, K.; et al. Metabolomics and integrated network analysis reveal roles of endocannabinoids and large neutral amino acid balance in the ayahuasca experience. *Biomed. Pharmacother.* **2022**, *149*, 112845. [CrossRef]
55. Sumner, L.W.; Amberg, A.; Barrett, D.; Beale, M.H.; Beger, R.; Daykin, C.A.; Fan, T.W.; Fiehn, O.; Goodacre, R.; Griffin, J.L.; et al. Proposed minimum reporting standards for chemical analysis Chemical Analysis Working Group (CAWG) Metabolomics Standards Initiative (MSI). *Metabolomics* **2007**, *3*, 211–221. [CrossRef] [PubMed]